

Brief report

Targeted disruption of the hepcidin 1 gene results in severe hemochromatosis

Jeanne-Claire Lesbordes-Brion, Lydie Viatte, Myriam Bennoun, Dan-Qing Lou, Guillemette Ramey, Christophe Houbron, Ghislaine Hamard, Axel Kahn, and Sophie Vaulont

We previously reported that mice made deficient for the transcriptional factor USF2 fail to express hepcidin 1 and hepcidin 2 genes as a consequence of targeted disruption of the *Usf2* gene lying just upstream in the locus. These mice developed an iron overload phenotype with excess iron deposition in parenchymal cells and decreased reticuloendothelial iron. At that time, although the role of USF2 was still confounding, we proposed

for the first time the role of hepcidin as a negative regulator of iron absorption and iron release from macrophages. Accordingly, we subsequently demonstrated that hyperexpression of *hepcidin 1*, but not *hepcidin 2*, resulted in a profound hypsideremic anemia. To analyze the consequences of *hepcidin 1* deletion on iron metabolism without any disturbance due to USF2 deficiency, we disrupted the *hepcidin 1* gene by targeting almost all the

coding region. Confirming our prior results, *Hepc1*^{-/-} mice developed early and severe multivisceral iron overload, with sparing of the spleen macrophages, and demonstrated increased serum iron and ferritin levels as compared with their controls. (Blood. 2006;108:1402-1405)

© 2006 by The American Society of Hematology

Introduction

Hepcidin is a small circulating 25-amino-acid cysteine-rich peptide first identified in human blood¹ and urine.² Hepcidin is the product of the *HAMP* gene, which consists of 3 exons and encodes a precursor protein of 84 aa (for a review see Nicolas et al³ and Ganz⁴). The hepcidin gene is expressed in the hepatocytes, secreted in the circulation, and cleared by the kidney. Whereas humans, rats, dogs, and pigs have a single *HAMP* gene, there are 2 duplicated genes in mice, *Hepc1* and *Hepc2*.^{5,6} In mammals, convincing evidence indicates that hepcidin constitutes the master regulator of iron homeostasis; the circulating peptide acts to limit gastrointestinal iron absorption and serum iron by inhibiting dietary intestinal iron absorption and iron recycling by the macrophages.⁷ As befits an iron-regulatory hormone, hepcidin synthesis is induced by iron stores and inflammation and inhibited by anemia and hypoxia.^{5,8-10} Most of the iron overload syndromes known to date (primary hemochromatosis and secondary iron overloads) imply a reduction of hepcidin secretion. In contrast, hypersecretion of hepcidin seems to play a determining role in anemia of inflammation (for a review see Ganz¹¹). Four years after the discovery of the peptide, its mechanism of action was elucidated.¹² To limit iron egress, hepcidin binds to ferroportin, the transmembrane iron transporter necessary for iron transfer out of intestinal epithelial cells and macrophages,¹³ thereby inducing its internalization and subsequent degradation, leading to decreased export of cellular iron.^{12,14,15}

Much of the data concerning the involvement of hepcidin in iron metabolism were initially generated in mouse models. We

previously reported that mice made deficient for the transcriptional factor USF2 fail to express either the *Hepc1* or *Hepc2* gene, as a consequence of targeted disruption of the *Usf2* gene lying just upstream of the hepcidin genes.⁷ These mice presented with increased liver iron levels and developed an iron overload phenotype similar to that observed in hereditary hemochromatosis, with increased circulating iron, increased transferrin saturation, and decreased reticuloendothelial iron. We assume that the phenotype was not due to USF2 deficiency since an independent *Usf2* knockout (KO) line expressed a normal amount of hepcidin mRNA and had normal iron metabolism.¹⁶ We thus proposed the role of hepcidin as a negative regulator of iron absorption and iron release from macrophages. This hypothesis was further supported by our demonstration that transgenic mice overexpressing *Hepc1* were born with severe iron deficiency.¹⁶ Interestingly, we recently showed that transgenic mice overexpressing *Hepc2* presented with normal iron metabolism, suggesting that only *Hepc1* is able to regulate iron homeostasis in mice.⁶

To analyze the consequences of *Hepc1* deletion on iron metabolism without any disturbance due to USF2 deficiency (only 10% of *Usf2*^{-/-} mice survive), we decided to disrupt the *Hepc1* gene by targeting deletion of exons 1 and 2 by classic homologous recombination. Homozygous mice presented with normal viability and developed multivisceral iron overload, with sparing of the spleen macrophages. The mutant mice also demonstrated increased serum iron and ferritin levels as compared with their controls. The

From the Institut Cochin, Département de Génétique, Développement et Pathologie Moléculaire; Institut National de la Santé et de la Recherche Médicale (INSERM) U567; Centre National de la Recherche Scientifique (CNRS); and Université Paris Descartes, Faculté de Médecine René Descartes, Paris, France.

Submitted February 10, 2006; accepted March 14, 2006. Prepublished online as *Blood* First Edition Paper, March 30, 2006; DOI 10.1182/blood-2006-02-003376.

J.-C.L.-B. and L.V. contributed equally to this work.

J.-C.L.-B. and L.V. designed and performed research, analyzed data, and

wrote the paper; M.B., D.-Q.L. and G.R. performed experiments; C.H. and G.H. provided technical support for ES cells and homologous recombination; A.K. analyzed data; and S.V. designed research, analyzed data, and wrote the paper.

Reprints: Sophie Vaulont, Institut Cochin, Faculté de Médecine Cochin Port Royal, 24, Rue du Faubourg Saint Jacques 75014 Paris, France; e-mail: vaulont@cochin.inserm.fr.

The publication costs of this article were defrayed in part by page charge payment. Therefore, and solely to indicate this fact, this article is hereby marked "advertisement" in accordance with 18 U.S.C. section 1734.

© 2006 by The American Society of Hematology

Hepc1 KO mouse model will facilitate investigation into the pathogenesis of iron overload in hemochromatosis and provide opportunities to evaluate therapeutic strategies for prevention or correction of iron overload.

Study design

Targeted disruption of the murine *Hepc1* gene

The gene-targeting vector was constructed by replacement of the 2 first exons and part of exon 3 of the *Hepc1* gene with a *hygromycin* cassette under the control of the *PGK* promoter. This cassette is flanked in the 5' direction by a 4.7-kb homologous arm and in the 3' direction by a 1.7-kb homologous arm. Isogenic homologous DNA arms were obtained by long-distance genomic polymerase chain reaction (PCR; Expand Long Template PCR System; Roche, Mannheim, Germany) using mouse 129/Sv genomic DNA as template and subcloned. Primers for PCR-made fragments were as follows: for the 5' homologous fragment (HF), forward 5'-CGGGGTACCTGATCAGAGTACCAGCCAGGACAGAGCC-3' and reverse 5'-CGGGGTACCTGGCTGTCTAGGAGCCAGTCCC-3' and for the 3' HF, forward 5'-ATTTGCGGCCGCTGCTGTAACAATTCCCAGTG-3' and reverse 5'-ATTTGCGGCCGCTGATCAGCTAGAAATCAAGAGGCCCTGG-3'. The 2 PCR-amplified homologous fragments were sequenced to confirm sequence fidelity. Details of vector construction are available on request. Linearized vector (25 µg) was electroporated into CK35 embryonic stem (ES) cells.¹⁷ Resistant clones were subjected to recombinant selection by PCR and correct recombination was further confirmed by Southern blot analysis. ES-cell clones with normal karyotypes were injected into C57BL/6 blastocysts and the obtained chimeric males were bred with C57BL/6 females to produce outbred F1 offsprings carrying the modified *Hepc1* allele. Subsequent genotyping was carried out by PCR analysis on DNA extracted from tail samples. Detailed information for genotyping is available on request. All the studies were carried out on F1 hybrids on a mixed C57BL/6 × 129 background.

Animals

All animals were cared for in accordance with the European convention for the protection of laboratory animals. Animals were maintained in a temperature- and light-controlled environment and were given free access to tap water and food (standard laboratory mouse chow, AO3, iron content 280 mg/kg; Usine d'Alimentation Rationnelle [UAR], Epinay-sur-Orsay, France). Iron overload was induced by adding 2% carbonyl iron (reduced pentacarbonyl iron) to the diet (AO3; UAR) for 14 days.

Hematologic analysis of mice

Blood was obtained by retro-orbital phlebotomy before killing of mice and collected in heparinized tubes (capiject T-MLH; Laboratoires Terumo, Guyancourt, France). Blood-cell counts and erythrocyte parameters were determined using a MaxM coulter automatic analyzer (Coulter, Hialeah, FL).

Reverse transcription and reverse transcriptase (RT)-PCR

Total RNA and double-stranded cDNA were prepared as previously described.⁷ PCR conditions were 25 cycles of denaturation at 94°C for 30 seconds, annealing at 50°C for 30 seconds, and primer extension at 72°C for 30 seconds. Following PCR, the amplified products (171 bp for *Hepc1* and *Hepc2* and 250 bp for *β-actin* and *Usf2*) were separated by electrophoresis on 1.5% agarose gel. Sequences of the primers were as follows: *Hepc1*, 5'-CCTATCTCCATCAACAGATG-3' (forward) and 5'-AACAGATACCACTGGGAA-3' (reverse); *Hepc2*, 5'-CCTATCTCCAGCAACAGATG-3' (forward) and 5'-AACAGATACCACAGGAGGGT-3' (reverse); *β-actin*, 5'-AGCCATGTACGTAGCCATCC-3' (forward) and 5'-TTTGATGT-CACGCACGATT-3' (reverse). For *Usf2*, the PCR conditions were the same except the annealing temperature was 55°C. The primers used were

as follows: 5'-TCATGCAGACAACAGCAAGACA-3' (forward) and 5'-TCACTGCCGGTACTCTCGC-3' (reverse).

Iron measurements and immunohistochemistry

Serum and tissue iron concentrations were determined as previously described¹⁸ using the "IL test" (Instrumentation Laboratory, Lexington, MA). For histology, tissues were fixed in 4% formaldehyde and embedded in paraffin. Sections were immersed in Perls solution (1:1, 2% HCl and 2% potassium ferrocyanide) to visualize ferric (non-heme) iron and counterstained with nuclear fast red using standard procedures. Quantification of serum ferritin levels was performed on an Olympus AU400 automat, using the Olympus human ferritin assay kit (Olympus, Hamburg, Germany).

Results and discussion

Targeted disruption of *Hepc1* results in the same iron disorders as those observed in *Usf2* KO mice. Targeted disruption of *Hepc1* was obtained by replacing exons 1 and 2 and part of exon 3 with a hygromycin resistance cassette using homologous recombination in ES cells. Correctly targeted clones were identified by Southern blot analysis (using the indicated 5' probe, Figure 1A) and PCR analysis (data not shown). Chimeric animals were bred with C57BL/6 females to produce inbred F1 offspring carrying the modified *Hepc1* allele. Germline transmission of the targeted allele was confirmed by PCR analysis (not shown). We interbred *Hepc1*^{+/-} animals to produce *Hepc1*^{-/-} offspring, and obtained approximately 25% *Hepc1*^{-/-} animals, indicating that there was no significant prenatal lethality. To assess the specificity of the *Hepc1* targeting deletion, we checked by RT-PCR the absence of *Hepc1* transcript in the liver of *Hepc1*^{-/-} animals (Figure 1B). Furthermore, we showed that, in contrast to the inhibition of *Hepc1* and *Hepc2* gene transcription observed in the *Usf2*^{-/-} mice, the expression of the neighboring genes of *Hepc1*, namely *Hepc2* and *Usf2*, were still expressed in *Hepc1*^{-/-} mice (Figure 1B). The mutant mice developed normally, showed no evidence of abnormalities, and both *Hepc1*^{-/-} females and males appeared fertile. The only visible phenotype was a statistical loss of body weight beginning at the age of 8 months (not shown). The hematologic parameters of the mutant mice were followed through development (red blood cell, hemoglobin, mean cell volume, and hematocrit); although they were slightly increased in the first months, all the indices returned to normal value at the age of 6 months (not shown). Tissue iron accumulation was assessed by Perls staining. As shown in Figure 1C, massive iron accumulation was present in the livers and pancreata of 4-month-old *Hepc1*^{-/-} mice and significant iron was also detected in the hearts. In contrast, splenic iron content was markedly decreased in *Hepc1*^{-/-} mice as compared with wild-type mice. Excess non-heme iron was also present in kidney, lung, muscle, and brain (data not shown). Further examination of liver iron accumulation showed that iron accumulated in liver parenchymal cells (hepatocytes), with sparing of the resident macrophages (Kupffer cells). Surprisingly, iron deposition was found more prominent in the centrilobular areas (Figure 1D, left panel). To determine whether this iron deposition was due to an intrinsic incapacity of *Hepc1*^{-/-} mice to load iron in the periportal region, control and mutant animals were given a 2% iron carbonyl-rich diet for 14 days. It is indeed well documented that dietary carbonyl iron overload is associated with specific iron deposition in the periportal hepatocytes. This periportal staining was evidenced in the experimentally iron-loaded control mice (Figure 1D) as well

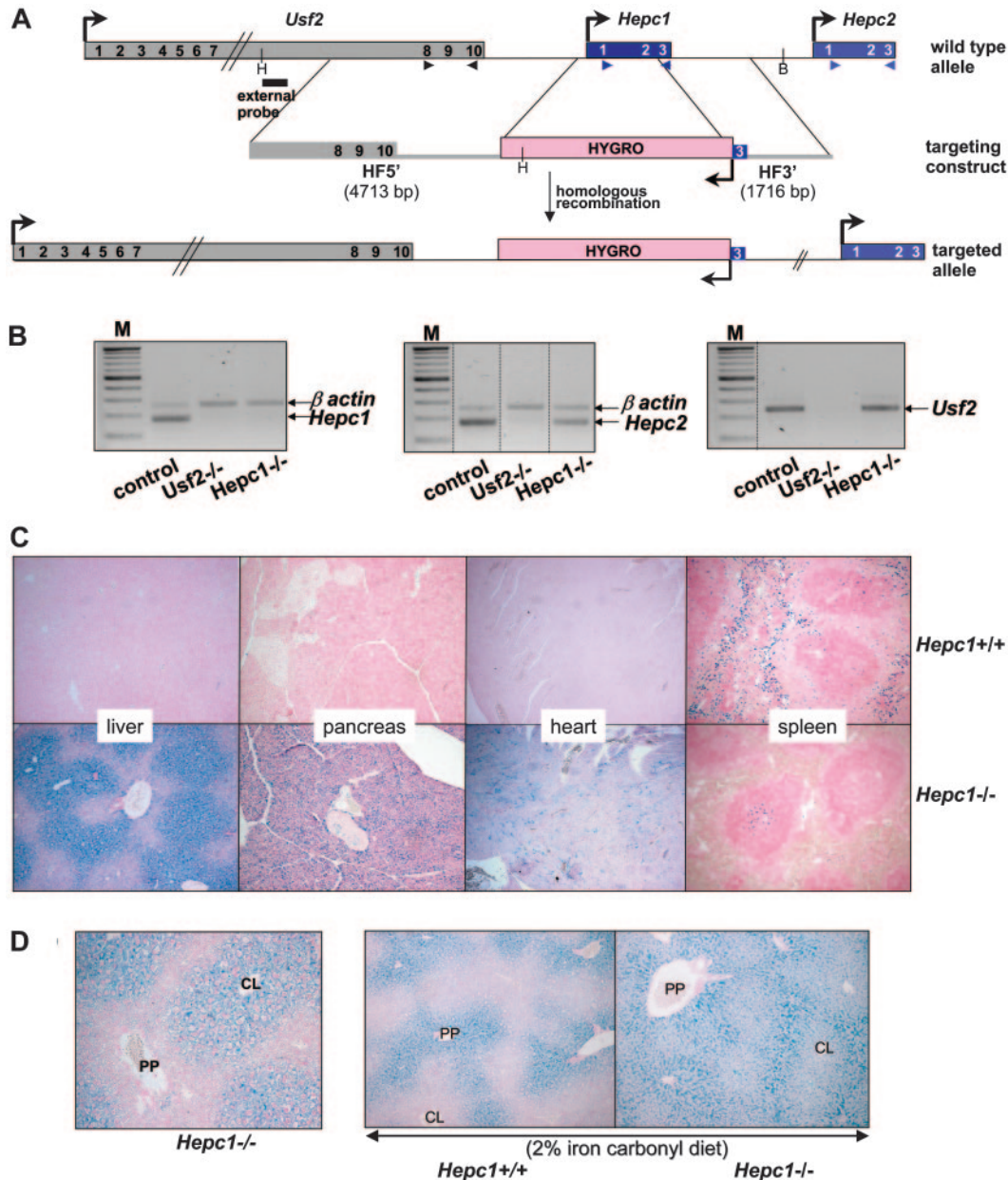
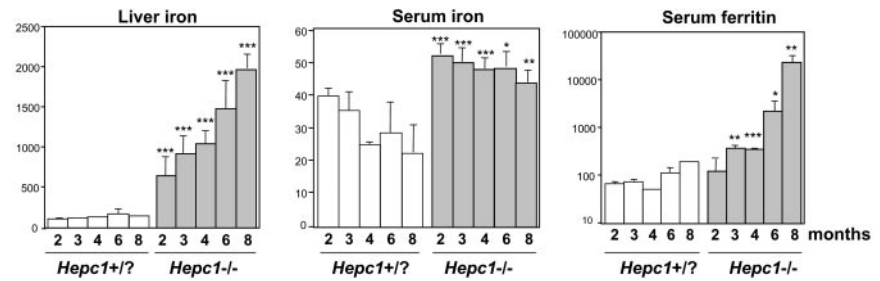


Figure 1. Generation of the *Hepc1* knockout mice and phenotypic exploration. (A) Schematic representation of the targeting strategy. The structure of the *Usf2/Hepc1/Hepc2* locus is shown at the top,⁶ the targeting construct in the middle and the resulting targeted allele at the bottom. The genes are represented by colored rectangles and the arrows represent the direction of the transcription. Restriction sites for *Hind*III (H) and *Bgl*III (B), used for Southern blot genotyping, and probe location are indicated. The arrowheads indicate the location of the primers designed for the RT-PCR (B). The scheme is not drawn to scale. HF indicates homologous fragments. (B) Level of specific *Hepc1*, *Hepc2*, and *Usf2* transcripts in the livers of controls, *Usf2*^{-/-} and *Hepc1*^{-/-} mice age 6 to 8 months, as measured by RT-PCR. Following PCR, the amplified products (171 bp for *Hepc1* and *Hepc2* and 250 bp for β -actin and *Usf2*) were separated by electrophoresis on 1.5% agarose gel. M indicates 100-bp DNA ladders. The vertical dotted lines indicate assembly of noncontiguous lanes. (C) Perls staining of liver, pancreas, heart, and spleen sections. Typical liver, pancreas, and spleen sections (original magnification $\times 10$) from *Hepc1*^{+/+} and *Hepc1*^{-/-} mice age 4 months. Non-heme iron stains blue. (D) Perls staining of liver sections (original magnification $\times 10$). Left, typical liver section of a 2-month-old *Hepc1*^{-/-} animal. CL, centrolobular; PP, periportal. Right, liver sections from 2-month-old *Hepc1*^{-/-} and *Hepc1*^{-/-} animals submitted to an iron-rich diet for 14 days.

as in the *Hepc1*^{-/-} mice, leading to a panlobular staining of the hepatic lobule of the mutant mice. We then examined the age-dependent variation of hematologic and iron parameters in control and *Hepc1*^{-/-} mice from 2 to 8 months of age. Controls consist of both *Hepc1*^{+/+} and *Hepc1*^{+/-} since no significant difference was observed between these animals. As shown in Figure 2, liver iron content was already 5-fold increased in 2-month-old mutant mice and continued to increase over the duration of the study. At 8 months, *Hepc1*^{-/-} mice had almost 15-fold more liver iron than control mice. At that age, mutant mice presented with a 30-fold

increase of iron in the pancreas (2056 ± 85 μ g iron/g of wet tissue in *Hepc1*^{-/-} mice, $n = 3$, versus 66 ± 6 in control mice, $n = 4$; $P < 10^{-7}$), a 5.5-fold increase in the heart (513 ± 145 μ g iron/g of wet tissue in *Hepc1*^{-/-} mice, $n = 3$, versus 92 ± 30 in control mice, $n = 4$; $P = .002$) whereas splenic iron was decreased by almost 3-fold (273 ± 30 μ g iron/g of wet tissue in *Hepc1*^{-/-} mice, $n = 3$, versus 784 ± 23 in control mice, $n = 4$; $P < .001$). Serum ferritin levels increased in parallel to the liver iron increase. In contrast, serum iron increased at 2 months and remained constant during the following months.

Figure 2. Age-dependent examination of hematologic and iron parameters. Liver iron (μg iron/g wet tissue), serum iron (μM), and ferritin (ng/mL) were determined in control (*Hepc1*^{+/+} and *Hepc1*^{+/-} mice) and *Hepc1*^{-/-} mice between 2 and 8 months of age. Statistical analysis was performed using Student *t* test (unpaired, 2-tailed). **P* < .05; ***P* < .01; ****P* < .001 as compared with sex- and age-matched animal; there were at least 5 animals in each group.



Collectively, these features of iron disorders observed in *Hepc1*^{-/-} mice appeared very similar to those described in the *Usp2*^{-/-} mice. They confirm our first hypothesis that iron deregulation of the *Usp2*^{-/-} mice was due to the suppression of *Hepc1* gene expression, and highlight the nonredundant role of *Hepc1* and *Hepc2* in mice.

The phenotype reported here for the *Hepc1*^{-/-} mice is very similar to the one recently reported for *Hjv*^{-/-} mice that presented with a complete deficit in hepcidin production.^{19,20} These 2 mouse models are characteristic of the severe, early onset of human juvenile hemochromatosis caused by mutations in the hemojuvelin gene and, more rarely, in the hepcidin gene (for a review see Roetto and Camaschella²¹). The gradual accumulation of liver iron in the

Hepc1^{-/-} mice suggests that hepcidin is the final setpoint regulator of iron homeostasis and that, in its absence, there is no effective regulatory mechanism to decrease iron uptake. This result differs from that observed in the *Hfe*^{-/-} mice, which do not completely lack hepcidin and still retain their ability to regulate intestinal iron absorption.²² The most intriguing result reported here, which seems in fact a unique feature of the *Hepc1*^{-/-} mice, is the centrolobular accumulation of liver iron. Indeed, when documented, the iron accumulation of the other forms of hemochromatosis, primary or secondary, appeared to be periportal. The specific zonation seen in *Hepc1*^{-/-} mice is interesting but difficult to explain. In this respect, it will be interesting to analyze the specific zonation of the iron-related proteins in the liver, a still poorly investigated domain.

References

- Krause A, Neitz S, Magert HJ, et al. LEAP-1, a novel highly disulfide-bonded human peptide, exhibits antimicrobial activity. *FEBS Lett*. 2000; 480:147-150.
- Park CH, Valore EV, Waring AJ, Ganz T. Hepcidin: a urinary antimicrobial peptide synthesized in the liver. *J Biol Chem*. 2001;276:7806-7810.
- Nicolas G, Viatte L, Bennoun M, Beaumont C, Kahn A, Vaulont S. Hepcidin, a new iron regulatory peptide. *Blood Cells Mol Dis*. 2002;29:327-335.
- Ganz T. Hepcidin, a key regulator of iron metabolism and mediator of anemia of inflammation. *Blood*. 2003;102:783-788.
- Pigeon C, Ilyin G, Courselaud B, et al. A new mouse liver specific gene, encoding a protein homologous to human antimicrobial peptide hepcidin, is overexpressed during iron overload. *J Biol Chem*. 2001;276:7811-7819.
- Lou DQ, Nicolas G, Lesbordes JC, et al. Functional differences between hepcidin 1 and 2 in transgenic mice. *Blood*. 2004;103:2816-2821.
- Nicolas G, Bennoun M, Devaux I, et al. Lack of hepcidin gene expression and severe tissue iron overload in upstream stimulatory factor 2 (USF2) knockout mice. *Proc Natl Acad Sci U S A*. 2001; 98:8780-8785.
- Nicolas G, Chauvet C, Viatte L, et al. The gene encoding the iron regulatory peptide hepcidin is regulated by anemia, hypoxia, and inflammation. *J Clin Invest*. 2002;110:1037-1044.
- Nemeth E, Valore EV, Territo M, Schiller G, Lichtenstein A, Ganz T. Hepcidin, a putative mediator of anemia of inflammation, is a type II acute-phase protein. *Blood*. 2003;101:2461-2463.
- Nemeth E, Rivera S, Gabayan V, et al. IL-6 mediates hypoferremia of inflammation by inducing the synthesis of the iron regulatory hormone hepcidin. *J Clin Invest*. 2004;113:1271-1276.
- Ganz T. Hepcidin—a regulator of intestinal iron absorption and iron recycling by macrophages. *Best Pract Res Clin Haematol*. 2005;18:171-182.
- Nemeth E, Tuttle MS, Powelson J, et al. Hepcidin regulates cellular iron efflux by binding to ferroportin and inducing its internalization. *Science*. 2004;306:2090-2093.
- Donovan A, Lima CA, Pinkus JL, et al. The iron exporter ferroportin (Slc40a1) is essential for iron homeostasis. *Cell Metabolism*. 2005;1:191-200.
- Knutson MD, Oukka M, Koss LM, Aydemir F, Wessling-Resnick M. Iron release from macrophages after erythrophagocytosis is up-regulated by ferroportin 1 overexpression and down-regulated by hepcidin. *Proc Natl Acad Sci U S A*. 2005;102:1324-1328.
- Delaby C, Pilard N, Goncalves AS, Beaumont C, Canonne-Hergaux F. The presence of the iron exporter ferroportin at the plasma membrane of macrophages is enhanced by iron loading and down-regulated by hepcidin. *Blood*. 2005;106: 3979-3984.
- Nicolas G, Bennoun M, Porteu A, et al. Severe iron deficiency anemia in transgenic mice expressing liver hepcidin. *Proc Natl Acad Sci U S A*. 2002;99:4596-4601.
- Kress C, Vandormael-Pourin S, Baldacci P, Cohen-Tannoudji M, Babinet C. Nonpermissiveness for mouse embryonic stem (ES) cell derivation circumvented by a single backcross to 129/Sv strain: establishment of ES cell lines bearing the Omd conditional lethal mutation. *Mamm Genome*. 1998;9:998-1001.
- Torrance JD, Bothwell TH. Tissue iron stores. *Methods Hematol*. 1980;1:90-115.
- Huang FW, Pinkus JL, Pinkus GS, Fleming MD, Andrews NC. A mouse model of juvenile hemochromatosis. *J Clin Invest*. 2005;115:2187-2191.
- Niederkofler V, Rishard S, Arber S. Hemojuvelin is essential for dietary iron-sensing and its mutation leads to severe iron overload. *J Clin Invest*. 2005;115:2180-2186.
- Roetto A, Camaschella C. New insights into iron homeostasis through the study of non-HFE hereditary haemochromatosis. *Best Pract Res Clin Haematol*. 2005;18:235-250.
- Ajioka RS, Levy JE, Andrews NC, Kushner JP. Regulation of iron absorption in Hfe mutant mice. *Blood*. 2002;100:1465-1469.